

## Optimization of Die Geometry for Tube Channel Pressing

M. H. Farshidi\*

Department of Materials Science and Metallurgical Engineering, Ferdowsi University of Mashhad, Azadi Square, Mashhad, Iran.

**Abstract:** Since tubes have numerous industrial applications, different attempts are focused on the severe plastic deformation processes of tubes. As an illustration, Tube Channel Pressing (TCP) is an attractive process for this purpose since it can be used to process different sizes of tubes. However, more attempts are needed to improve the outcomes of TCP. For example, the imposition of a greater strain besides reductions in the strain heterogeneity are the challenges of this process. This work is aimed to optimize the die geometry of TCP through a finite element simulation procedure verified by experiments in order to increase the imposed strain as well as decreasing the strain heterogeneity. Results show that the increase in die curvature radius causes the reduction of imposed plastic strain and an increase in strain heterogeneity. In addition, the minimum amount of die convex height for the imposition of a reasonable strain through TCP is calculated considering the tube thickness and the channel angle. In addition to this, the optimum die geometry is recommended in order to minimize the strain heterogeneity.

**Keywords:** Severe plastic deformation, Finite element simulation, Strain analysis.

### 1. Introduction

The imposition of Severe Plastic Deformation (SPD) is considered an attractive method for the improvement of mechanical properties and grain refinement of metallic materials. For example, Equal Channel Angular Pressing (ECAP) for rods, High Pressure Torsion (HPT) for thin disks and Accumulative Roll Bonding (ARB) for sheets are well-known SPD processes developed during past decades [1-4]. Recently, different works have focused on the development of SPD processes for tubes in basis of ARB, HPT, and ECAP [4-11]. In comparison with other processes, SPD processes for tubes developed in basis of ECAP have various benefits such as: less limitation for the dimensions of tubes, the necessity of less complicated machinery device and the imposition of a relatively homogenous plastic strain. Examples of these processes can be presented as: tubular ECAP [7-8], Tube Channel Pressing (TCP) [9-11], and Tubular Channel Angular Pressing (TCAP) [12-13]. To elaborate on the matter consider that when a tube is processed by TCP, it passes a bottleneck region which causes a multi-stage shear straining and hoop straining as shown in Fig. 1 [9-10]. Although a few studies have focused on the effect of die/mandrel geometry on the deformation behavior of tubes through TCP [10-11, 14], some aspects of TCP die geometry have remained less considered. As an illustration of this note that previous studies have shown a considerable heterogeneity of strain imposed by this process which is not desirable for an SPD process. Besides this, the effect of die geometry on the imposed strain through TCP has not been yet studied thoroughly. Therefore, more attempts are needed to decrease the strain heterogeneity and to analyze the amount of strain imposed by this process.

The aim of this work is to decrease the strain heterogeneity and increase the imposed strain of TCP process through the optimization of new die geometry. For this purpose, a Finite Element Method (FEM) simulation procedure is applied to predict the deformation behavior of Al-1.7Fe-0.9Si-0.5Cu tube through

processing by different TCP dies. Besides this, experimental examinations are accomplished using a TCP die to investigate the accuracy of simulation results. Comparing the results of simulations and those of experiments, the geometry of die is optimized to minimize the strain heterogeneity and to impose a greater strain.

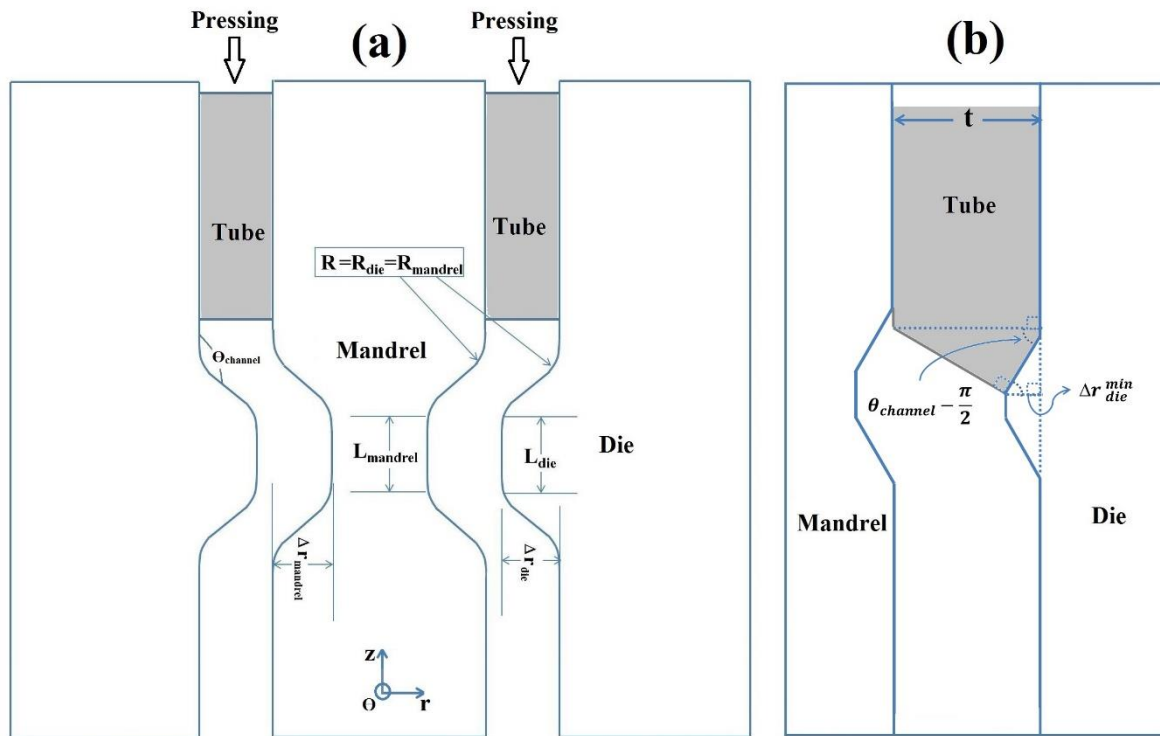


Fig. 1. (a) Schematic illustration of the new geometry of TCP and its geometrical variables. (b) The illustration of the minimum of  $\Delta r_{die}$  for the occurrence of subsequent shear through TCP.

## 2- Analysis and Selection of Parameters for TCP

Figure 1 shows a schematic illustration of a new geometry of TCP process and its die/mandrel geometrical parameters. As can be seen, the processing of a tube by the new geometry of TCP causes four stages of shear straining of tube wall besides two stages of hoop straining. Considering constant dimensions of one tube, geometrical variables of TCP process are as follows: the channel angle ( $\theta_{channel}$ ), the length of mandrel cave ( $L_{mandrel}$ ), the curvature radii of die/mandrel ( $R$ ), the height of die convex ( $\Delta r_{die}$ ), and the depth of mandrel cave ( $\Delta r_{mandrel}$ ). In this work, the inner and outer diameters of the used tube are 44.4 and 50.8 mm, respectively. This clarifies a tube thickness ( $t$ ) of 3.2 mm. Considering previous studies,  $\theta_{channel}$  and  $L_{die}$  are constantly considered as  $150^\circ$  and 0 mm while  $L_{mandrel}$  is considered as 2 mm regarding the thickness of the used tube [10-13]. In addition, to avoid the thinning of the tube over TCP processing as much as possible, the cross section area of the tube in the middle of the bottleneck region shall not be reduced. Therefore, the depth of mandrel cave ( $\Delta r_{mandrel}$ ) is calculated according to Eq. (1) [14]:

$$r_{Ot}^2 - r_{It}^2 = (r_{Ot} - \Delta r_{die})^2 - (r_{It} - \Delta r_{mandrel})^2 \quad (1)$$

Here,  $r_{Ot}$  is the outer radius of tube and  $r_{It}$  is its inner radius.

With regard to what told above, one die geometry can be characterized by two independent geometrical variables: curvature radius ( $R$ ) and die convex height ( $\Delta r_{die}$ ). As shown before, the corner of the channel of TCP die shall be smooth to avoid the stress concentration on die as well as preventing deviated shapes of the tube after the process [11]. On the other hand, selection of a large curvature radius increases the heterogeneity of the imposed strain through TCP [15]. With regard to these limitations, six

different amounts of 0.8, 1.6, 2.4, 3.2, 4 and 4.8 mm ( $\approx 0.25, 0.5, 0.75, 1, 1.25$  and  $1.5$  times of tube thickness) are selected for  $R$  of TCP to evaluate the effect of this variable on the deformation behavior of the tube.

Considering the ideal geometry of TCP shown in Fig. 1b, one may relate the minimum of  $\Delta r_{die}$  for the occurrence of subsequent shear in tube wall to  $\Theta_{channel}$  and  $t$  as follows:

$$\Delta r_{die}^{min} = t \cos^2 \left( \Theta_{channel} - \frac{\pi}{2} \right) \quad (2)$$

By substituting  $\Theta_{channel}$  and having  $t$  equal to  $150^\circ$  and 3.2 mm,  $\Delta r_{die}^{min}$  is calculated as 0.8 mm ( $0.25t$ ). It is noteworthy that the imposed strain through a shear by the channel angle of  $\Theta_{channel}$  can be calculated as follows [4]:

$$\varepsilon = 1.15 \text{Cot} \left( \frac{\Theta_{channel}}{2} \right) \quad (3)$$

Similarly, the hoop strain by changing tube radius from  $r_1$  to  $r_2$  can be calculated as follows [9]:

$$\varepsilon = 1.15 \text{Ln} \left( \frac{r_1}{r_2} \right) \quad (4)$$

Therefore, by considering four stages of shear straining and two stages of hoop straining through TCP, the total equivalent plastic strain on each selected element of tube wall can be analytically calculated as:

$$\varepsilon = 1.15 \left\{ 4 \text{Cot} \left( \frac{\Theta_{channel}}{2} \right) + 2 \text{Ln} \left( \frac{r_{tube}}{r_{bottleneck}} \right) \right\} \quad (5)$$

Here,  $r_{tube}$  and  $r_{bottleneck}$  are the radii of the selected element before the process and in the middle of bottleneck zone, respectively. According to Eq. (5), the amount of the imposed strain increases by the increase of  $\Delta r_{die}$  (see Fig. 1 & Eq. (1)). It is notable that greater hoop strains are imposed on the inner side of the tube compared to what is imposed on the outer side of the tube since the relative variation of inner radius of the tube through TCP is greater than the relative variation of outer radius of the tube according to Eq. (1). Moreover, by an increase of  $\Delta r_{die}$ , the relative increase of  $\Delta r_{mandrel}$  is greater than that of  $\Delta r_{die}$  according to Eq. (1). Therefore, the heterogeneity of hoop strains increases by an increase of  $\Delta r_{die}$ .

Although the effect of  $\Delta r_{die}$  on the deformation behavior of the tube is briefly explained in the previous paragraph, it must be mentioned that the presented analysis considers the ideal shear straining and hoop straining through TCP which occur by selecting a sharp channel corner. Therefore, the presented analysis may not be true for a real TCP die which has a smooth channel corner. In other words, since the channel corner of a real TCP die is relatively smoothed by a curvature radius of  $R$ , the effect of  $\Delta r_{die}$  on the deformation behavior of the tube through TCP may be dependent on  $R$ . Regarding this, seven different amounts of 0.5, 0.9, 1.3, 2.1, 3.1, 4.1 and 5.1 mm ( $\approx 0.16, 0.28, 0.41, 0.65, 0.97, 1.28$  and  $1.6$  times of  $t$ ) are selected for  $\Delta r_{die}$  to investigate the effect of this variable on the deformation behavior of the tube through TCP processing.

### 3. Simulation Procedure

Deformation behavior of Al-1.7Fe-0.9Si-0.5Cu alloy tube during processing by different TCP dies is simulated by Abaqus 6.13 software using a 2D axisymmetric dynamic explicit model based on Lagrangian formulation. The adaptive meshing method is applied to decrease the mesh distortion during simulation. Die and mandrel are meshed using the CAX3 and CAX4R elements which respectively consist of 3 and 4 nodes. The mesh sizes for these parts are as follows: 7 mm for surfaces which have no contact with the specimen, 2 mm for surfaces which have contact with the specimen out of the bottleneck zone, and 0.5 mm for surfaces which have contact with the specimen inside of the bottleneck zone. The specimen is meshed using 1080 number of  $0.5 \times 0.5$  mm CAX4R elements. To investigate the mesh sensitivity of the applied simulation method, one simulation was carried out using a mesh size half of the mentioned

amounts. Results of this simulation have shown a negligible difference compared to the results of its counterpart using the typical mesh size. For example, the difference in the calculated equivalent plastic strain was less than 5%. The interaction between die, mandrel, and specimen surfaces is defined by the penalty contact method and the sliding friction coefficient is considered equal to 0.01. Voce relation is used for the extrapolation of flow stress vs. plastic strain curve since this relation can accurately predict this curve for aluminum alloys subjected to extensive plastic strains [16-17]. Using this relation, the amount of flow stress ( $\sigma_{flow}$ ) after the imposition of plastic of  $\varepsilon_p$  is as follows:

$$\sigma_{flow} = \sigma_{\infty} - (\sigma_{\infty} - \sigma_0) \exp(-c\varepsilon_p) \quad (6)$$

Here,  $\sigma_0$ ,  $\sigma_{\infty}$  and  $c$  are constants of the relation. These parameters are calculated by fitting the results of a tension test of the used alloy and those of a previous experiment on the flow stress of a similar alloy after SPD processing [18].

#### 4. Experiments and Validation Procedure

The tube is received in wrought form and cut to 90 mm specimens. These specimens are annealed for 45 min. in 753 K to eliminate the probable work hardening of material through previous tube forming process. Then, a tensile test is achieved to obtain flow stress vs. plastic strain curves for the used alloy. A TCP die is manufactured using the  $R$  of 3.2 mm and  $\Delta r_{die}$  of 3.1 mm and this die is used for experimental studies on the deformation behavior of the tube. As shown in Fig. 2, the contact surfaces of die/mandrel with specimen are fully polished to decrease the friction coefficient as much as possible. In addition, MoS<sub>2</sub> aerosol is used for the lubrication of die, mandrel and specimen surfaces. In order to examine the capability of simulation procedure to estimate the needed deformation load of TCP, the experimentally obtained load-displacement curve through TCP of the used tube is compared with its simulated counterpart. Besides this, in order to study the ability of the simulation procedure to estimate the imposed plastic strain, variations of the Vickers hardness and the simulated imposed plastic strain along the tube wall thickness are compared. The Vickers hardness is obtained using 2 N load along the thickness of the TCP processed tube by the step distance of 0.5 mm.

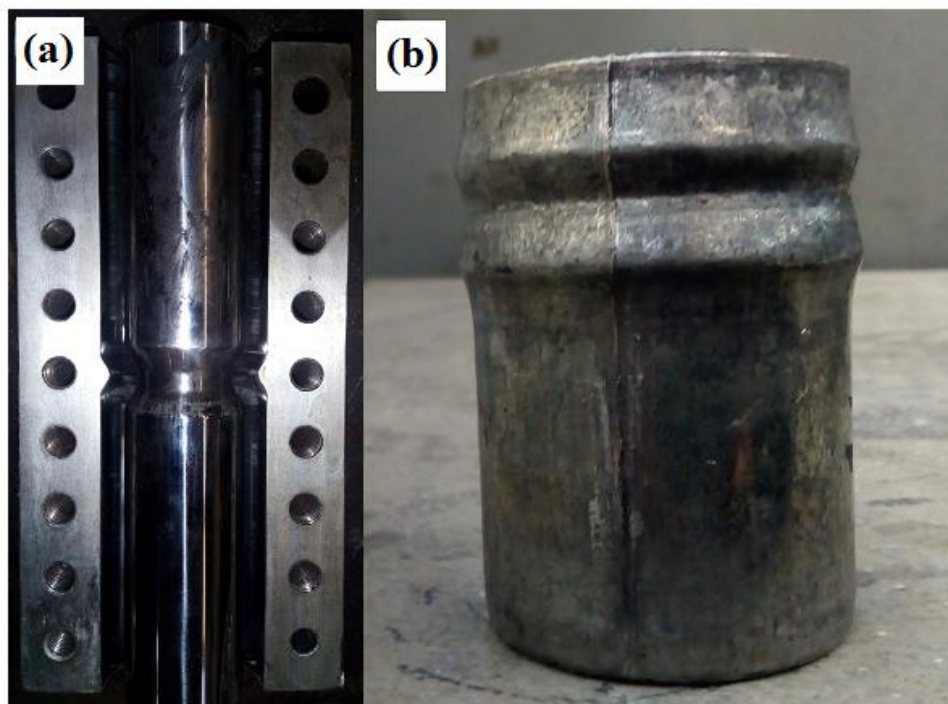


Fig. 2. (a) Manufactured TCP die. (b) A specimen processed using the manufactured die.

## 5. Results and Discussion

Figure 3a shows the simulated deformation behavior of the tube while being processed by TCP using the manufactured die. As can be seen, three different regions along tube length can be categorized considering the distribution of the imposed strain. At the bottom of the tube, the unsteady-state deformed region exists which has freely passed the bottleneck zone because of little frictional contact with die/mandrel surfaces. Since this region of the processed tube doesn't completely follow the channel route, the amount of the imposed strain on this region is relatively lower and its strain distribution is more heterogeneous in comparison with its upper counterpart. The middle region of the TCP processed tube is the steady-state deformed region which has been almost in full contact with die/mandrel surfaces during the deformation. As can be seen, a remarkable and relatively homogeneous strain is imposed on this region of the tube wall. The most upper region has remained in the bottleneck zone of the die after the process and hasn't finished the process. Therefore, the amount of the imposed strain on this region is relatively lower. It is also notable that since the next pass of TCP is imposed from the bottom of the tube up to its top, the unsteady-state deformed region and the remained region in bottleneck zone nearly replace each other in the next pass. This means limited involvement of these regions in the process. Thus, it is clear that the only usable section of a TCP processed tube is the steady-state deformed region whereas a considerable plastic strain is imposed almost homogeneously. Therefore, analysis of the imposed strain and the strain heterogeneity is focused on this region.

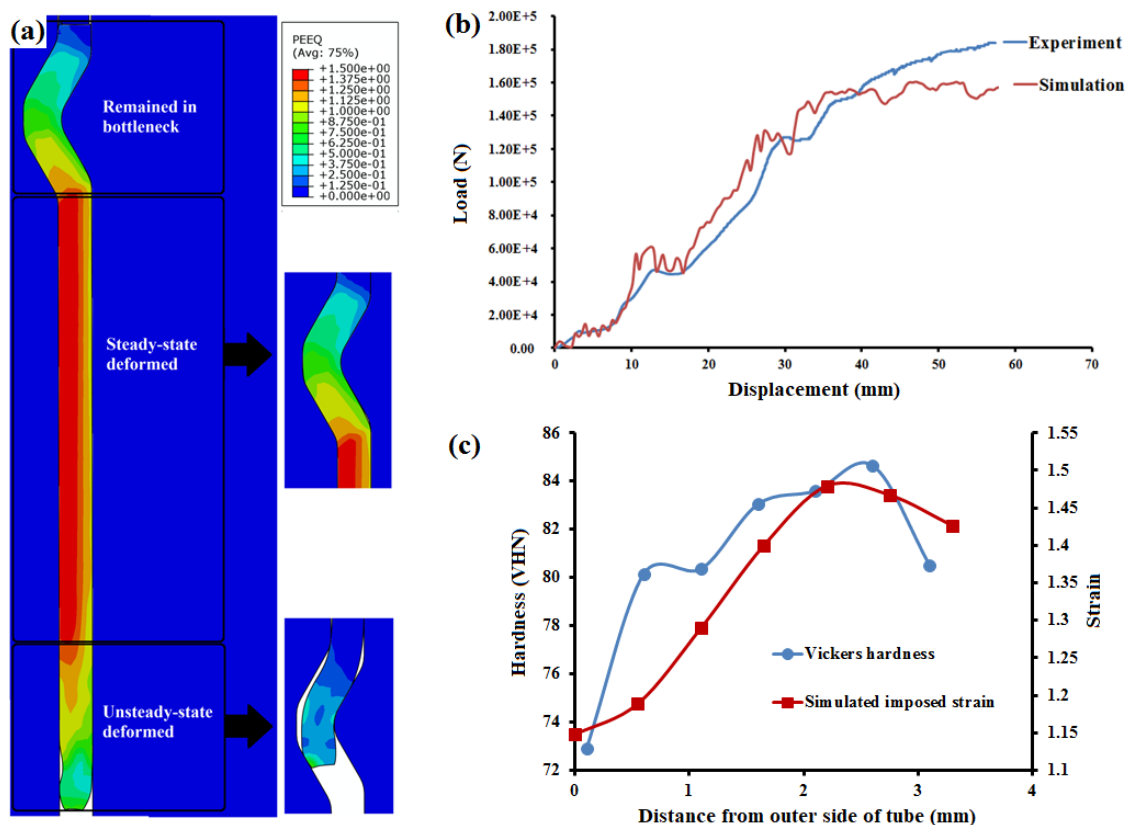


Fig. 3. (a) Illustration of three differently deformed regions through processing by TCP. (b) Comparison of simulation and experiment results for load-displacement curve through TCP processing using the manufactured die. (c) Comparison of the simulated imposed strain and the Vickers micro-hardness along the tube wall thickness after one pass of TCP.

Figure 3b compares the experimentally obtained deformation load with displacement through TCP processing using the manufactured die by its simulated counterpart. As can be seen, the general trend of

experimentally obtained deformation load follows its simulated counterpart. Figure 3c compares variation of the Vickers micro-hardness along the tube thickness with simulated imposed plastic strain through TCP processing. As shown here, the Vickers hardness variation trend is comparable with that of the imposed plastic strain. Considering these results, the capability of simulation procedure to estimate both deformation load and imposed plastic strain is verified.

Figure 4a compares the variation of the imposed plastic strain through TCP processing with variation of curvature radius ( $R$ ) and convex height of die ( $\Delta r_{die}$ ). Equation (5) is applied to obtain an analytical approximation of the imposed strain on the tube wall. For this purpose,  $\gamma_{tube}$  is considered as the average of inner and outer radii of the tube before the process and  $\gamma_{bottleneck}$  is considered as the average of inner and outer radii of the tube in the middle of the bottleneck zone. As shown in Fig. 4a, the imposed plastic strain decreases by the increase of  $R$  which will be discussed later. Moreover, the imposed plastic strain increases by the increase of  $\Delta r_{die}$  which can be attributed to the increase of the imposed hoop strain according to Eq. (5). It is also notable that the imposed strain by using  $\Delta r_{die}$  of 0.5 mm is much lower than what is approximated by Eq. (5). This implies a different deformation behavior of the tube using  $\Delta r_{die}$  of 0.5 mm which will be discussed later. Figure 4b compares the variation of the needed deformation load by the variation of  $R$  and  $\Delta r_{die}$ . As can be seen, the needed deformation load increases by a decrease of  $R$  and an increase of  $\Delta r_{die}$ . By comparing Figs. 4a & b, it is inferred that the variations of the needed deformation load and the imposed plastic strain through TCP processing are almost similar. Therefore, the increase of the deformation load by decreasing  $R$  and increasing  $\Delta r_{die}$  is mainly attributed to the increase of the imposed plastic strain as discussed before.

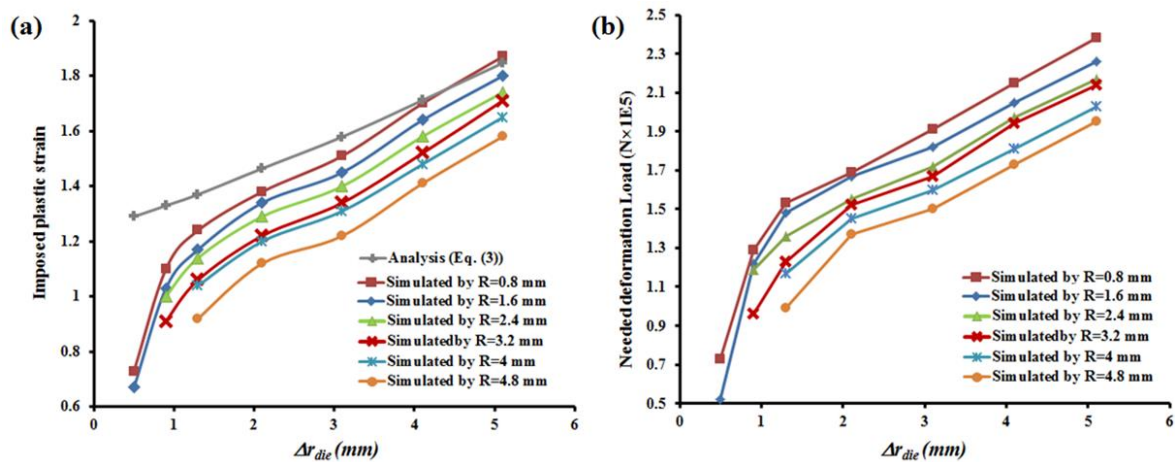


Fig. 4. The effect of  $\Delta r_{die}$  and  $R$  on: (a) Imposed plastic strain and (b) needed deformation load through TCP processing.

Figure 5 shows the effect of  $R$  and  $\Delta r_{die}$  on “Standard Deviation of strain distribution per unit of average Plastic Strain (SDPS)” which is calculated as follows:

$$SDPS = \frac{\sqrt{\frac{\sum_{i=1}^n (\varepsilon_i - \bar{\varepsilon})^2}{n}}}{\bar{\varepsilon}} \quad (7)$$

Here,  $n$  is the number of nodes along the tube thickness,  $\bar{\varepsilon}$  is the average of the imposed plastic strain and  $\varepsilon_i$  is the imposed strain on each node. It is notable that the nodes placed on the boundary of the tube are considered with coefficient of 0.5 in the calculation of  $\bar{\varepsilon}$  and SDPS. As shown in Fig. 5, the SDPS generally increases by the increase of  $R$ . For instance, the lowest SDPS is achieved by selecting  $R$  equal to 0.8-1.6 mm (0.25t-0.5t). In addition, variation of SDPS versus  $\Delta r_{die}$  has two different trends. While during the first step the SDPS decreases by increasing  $\Delta r_{die}$ , it increases by increasing  $\Delta r_{die}$  during the second step.

It is also noteworthy that the decrease of SDPS during the first step has two different rates: it drastically falls by the increase of  $\Delta r_{die}$  from 0.5 mm to 0.9 mm, while it decreases slightly by the increase of  $\Delta r_{die}$  from 0.9 mm. This implies a different deformation behavior of the tube through TCP processing when  $\Delta r_{die}$  of 0.5 mm is used which will be discussed later.

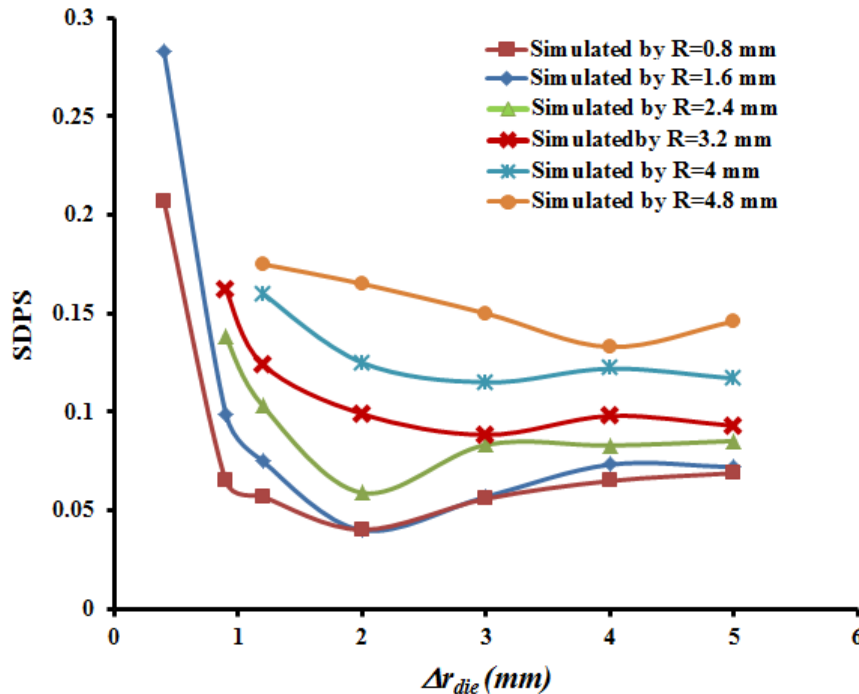


Fig. 5. The effect of  $\Delta r_{die}$  and  $R$  on variation of the SDPS through TCP processing.

Considering what told above, one can infer that the increase of  $R$  decreases the imposed plastic strain, while it increases the strain heterogeneity. Similarly, it has been reported that the increase of die corner radius of the ECAP process causes the decrease of the imposed plastic strain and the increase of strain heterogeneity. This effect has been attributed to the occurrence of bending instead of pure shear through the process [19-21]. As can be seen in Figs. 4 & 5, the effect of  $R$  on the strain heterogeneity is more severe than its effect on the imposed plastic strain. As an illustration of this; while the increase of  $R$  from 1.6 mm to 4.8 mm causes a few tens percent decrease of the imposed strain, it causes a few times increase of the SDPS. This severe increase in strain heterogeneity causes the heterogeneity of the properties of the processed tube, which is undesirable. Therefore, it seems that selecting  $R$  about  $0.25t-0.5t$  is more rational to obtain a relatively homogenous plastic strain.

As shown in Figs. 4 & 5, when  $\Delta r_{die}$  of 0.5 mm is selected for a die, the imposed strain is remarkably lower, while SDPS is impressively greater in comparison to other dies designed by greater amounts of  $\Delta r_{die}$ . As mentioned before, the  $\Delta r_{die}^{min}$  for the occurrence of subsequent shears in the tube wall through TCP processing can be analytically evaluated as 0.8 mm. The greater SDPS and the lower imposed strain on the tube wall by using  $\Delta r_{die}$  of 0.5 mm for TCP dies shown by simulations verify the accuracy of this definition of  $\Delta r_{die}^{min}$ . For more explanation, when  $\Delta r_{die}$  is selected less than  $\Delta r_{die}^{min}$ , the occurrence of shear in the tube wall is incomplete. This decreases the imposed strain and increases the SDPS. Besides this, although it was expected that the increase of  $\Delta r_{die}$  results in an increase of strain heterogeneity, this effect only occurs after a specific  $\Delta r_{die}$ . In other words, there is an optimum amount of  $\Delta r_{die}$  in which the SDPS is minimized and this optimum amount is dependent on  $R$ . As an illustration of this; when  $R$  of 4.8 mm is selected, the SDPS is minimized using  $\Delta r_{die}$  of 4.1 mm ( $1.28t$ ). Despite this, when  $R$  of 0.8-2.4 mm is selected, the SDPS is minimized using  $\Delta r_{die}$  of 2.1 mm ( $0.65t$ ). Considering these arguments, one can

propose that the geometry of a TCP die can be optimized by the selection of  $R$  and  $\Delta r_{die}$  about  $0.25t-0.5t$  and  $0.65t$  respectively to obtain the lowest strain heterogeneity besides a remarkable imposed plastic strain.

## 6. Conclusion

Considering the results of this work, it can be concluded that:

- 1- The applied simulation procedure can be used to predict the imposed plastic strain as well as the needed deformation load through TCP processing.
- 2- Increase of die curvature radius ( $R$ ) from 0.25-0.5 time of the tube thickness ( $t$ ) causes the decrease of the imposed plastic strain and the needed deformation load, while it increases the strain heterogeneity.
- 3- Considering the channel angle ( $\theta_{channel}$ ) equal to  $150^\circ$ , the minimum amount of die convex height ( $\Delta r_{die}$ ) for the occurrence of subsequent shears through TCP processing is obtained equal to  $0.25t$  as illustrated in Eq. (2).
- 4- The optimum amount of  $\Delta r_{die}$  is strongly dependent on  $R$ . For instance, by selecting  $R$  and  $\Delta r_{die}$  equal to  $0.25t-0.5t$  and  $0.65t$  respectively, the die geometry can be manipulated to obtain the minimum of strain heterogeneity besides a remarkable imposed plastic strain.

**Acknowledgements:** The author wishes to thank the research board of Ferdowsi University of Mashhad (FUM) for the financial support and the provision of research facilities used in this work through the project number of 2/37062.

## References

- [1] V.M. Segal, Material processing by simple shear, *Material science Engineering A*. 197 (1995) 157–164.
- [2] R.Z. Valiev, N.A. Krasilnikov, N.K. Tsenev, Plastic deformation of alloys with submicron-grained structure, *Materials Science Engineering A*. 137 (1991) 35-40.
- [3] N. Tsuji, Y. Saito, H. Utsunomiya, S. Tanigawa, Ultrafine grained bulk steel produced by Accumulative Roll-Bonding (ARB) process, *Scripta Materialia* 40 (1999) 795–800.
- [4] Y. Estrin, A. Vinogradov, Extreme grain refinement by severe plastic deformation: A wealth of challenging science, *Acta Materialia* 61 (2013) 782–817.
- [5] M.S. Mohebbi, A. Akbarzadeh, Accumulative spin bonding (ASB) as a novel SPD process for fabrication of nanostructured tubes, *Materials Science Engineering A* 528 (2010) 180–188.
- [6] L.S. Toth, M. Arzaghi, J.J. Fundenberger, B. Beausir, O. Bouaziz, R.A. Massion, Severe plastic deformation of metals by high-pressure tube twisting, *Scripta Materialia* 60 (2009) 175–177.
- [7] A.V. Nagasekhar, U. Chakkingal, P. Venugopal, Candidature of equal channel angular pressing for processing of tubular commercial purity-titanium, *Journal of Materials Processing Technologies*, 173 (2006) 53–60.
- [8] A.V. Nagasekhar, U. Chakkingal, P. Venugopal, Equal Channel Angular Extrusion of Tubular Aluminum Alloy Specimens—Analysis of Extrusion Pressures and Mechanical Properties, *Journal of Manufacturing Processes* 8 (2006) 112-120.
- [9] A. Zangiabadi, M. Kazeminezhad, Development of a Novel Severe Plastic Deformation Method for Tubular Materials: Tube Channel Pressing (TCP), *Materials Science and Engineering A* 528 (2011) 5066-5072.
- [10] M.H. Farshidi, M. Kazeminezhad, The effects of die geometry in tube channel pressing: Severe plastic deformation, *Journal of Materials: Design and Application* 230 (2016) 263–272.
- [11] M.H. Farshidi, New geometry for TCP: severe plastic deformation of tubes, *Iranian Journal of Materials Forming* 3 (2016) 64-78.



- [12] M. Javidikia, R. Hashemi, Analysis and Simulation of Parallel Tubular Channel Angular Pressing of Al 5083 Tube, *Transaction of the Indian Institute of Metals*, accepted and awaiting publishing, DOI: 10.1007/s12666-017-1117-7.
- [13] G. Faraji, F. Reshadi, M. Baniasadi, A New Approach for Achieving Excellent Strain Homogeneity in Tubular Channel Angular Pressing (TCAP) Process, *Journal of Advanced Materials and Processing* 2 (2014) 3-12.
- [14] M.H. Farshidi, M. Kazeminezhad, Deformation behavior of 6061 aluminum alloy through tube channel pressing: Severe plastic deformation, *Journal of Materials Engineering and Performance* 21 (2012) 2099–2105.
- [15] M.H. Farshidi, M. Kazeminezhad, H. Miyamoto, Microstructural evolution of aluminum 6061 alloy through Tube Channel Pressing, *Materials Science and Engineering A* 615 (2014) 139-147.
- [16] M. Kazeminezhad, E. Hosseini, Modeling of induced empirical constitutive relations on materials with FCC, BCC, and HCP crystalline structures: severe plastic deformation, *International Journal of Advanced Manufacturing Technologies* 47 (2010) 1033–1039.
- [17] A. Kacem, A. Krichen, P.Y. Manach, S. Thuillier, J.W. Yoon, Failure prediction in the hole-flanging process of aluminium alloys, *Engineering Fracture Mechanics* 99 (2013) 251–265.
- [18] M. Reihanian, R. Ebrahimi, M.M. Moshksar, D. Terada, N. Tsuji, Microstructure quantification and correlation with flow stress of ultrafine grained commercially pure Al fabricated by equal channel angular pressing (ECAP), *Materials Characterization* 59 (2008) 1312–1323.
- [19] N. Medeiros, L.P. Moreira, J.D. Bressan, J.F.C. Lins, J.P. Gouvea, Upper-bound sensitivity analysis of the ECAE process, *Materials Science and Engineering A* 527 (2010) 2831–2844.
- [20] C.J. Luis Perez, On the correct selection of the channel die in ECAP processes, *Scripta Materialia* 50 (2004) 387–393.
- [21] V. Patil Basavaraj, U. Chakkingal, T.S. Prasanna Kumar, Effect of geometric parameters on strain, strain inhomogeneity and peak pressure in equal channel angular pressing – A study based on 3D finite element analysis, *Journal of Manufacturing Process* 17 (2015) 88–97.

## بهینه سازی هندسه فرآیند فشار در کانال لوله‌ای

محمد حسن فرشیدی

گروه مهندسی متالورژی و مواد، دانشکده مهندسی دانشگاه فردوسی مشهد، مشهد، ایران

**چکیده:** بدلیل آنکه لوله‌ها کاربردهای صنعتی گوناگونی دارند، پژوهش‌های مختلفی جهت اعمال تغییر شکل مومسان شدید بر روی آن‌ها انجام شده است. به عنوان نمونه، فرآیند "فشار در کانال لوله‌ای"<sup>1</sup> به عنوان یک فرآیند قابل توجه در این زمینه مطرح شده است چراکه می‌تواند برای ابعاد گوناگون لوله‌ها مورد استفاده قرار گیرد. با این حال، پژوهش‌های بیشتری باید جهت بهینه‌سازی این فرآیند صورت پذیرد. به عنوان نمونه، اعمال کرنش‌های بزرگ به همراه کاهش ناهمگنی کرنش، چالش‌هایی در این فرآیند هستند. هدف این پژوهش، بهینه کردن هندسه فرآیند فشار در کانال لوله‌ای از طریق انجام شبیه سازی اجزای محدود معتبر شده توسط آزمایشات عملی می‌باشد تا از این طریق، ناهمگنی کرنش اعمالی کاهش یافته و میزان کرنش اعمالی، افزایش یابد. نتایج نشان داد که با افزایش شعاع گوشه قالب، کرنش اعمالی کاهش یافته و ناهمگنی کرنش، بیشتر می‌گردد. به علاوه، حداقل میزان پیش آمدگی قالب جهت اعمال کرنشی قابل توجه، بر حسب ضخامت لوله و زاویه کانال بدست آمد. همچنین هندسه قالب بهینه جهت کاهش ناهمگنی کرنش، پیشنهاد گردید.

**واژه های کلیدی:** تغییر شکل مومسان شدید، شبیه سازی اجزای محدود، تحلیل کرنش.

<sup>1</sup> Tube Channel Pressing (TCP)